

**A GRIDLESS EULER/NAVIER-STOKES SOLUTION
ALGORITHM FOR COMPLEX TWO-DIMENSIONAL
APPLICATIONS**

JOHN T. BATINA

JUNE 1992

(NASA-TM-107631) A GRIDLESS
EULER/NAVIER-STOKES SOLUTION
ALGORITHM FOR COMPLEX
TWO-DIMENSIONAL APPLICATIONS
(NASA) 25 p

N92-30570

Unclass

63/02 0106618



National Aeronautics and
Space Administration
Langley Research Center
Hampton, Virginia 23665-5225

A GRIDLESS EULER/NAVIER-STOKES SOLUTION ALGORITHM FOR COMPLEX TWO-DIMENSIONAL APPLICATIONS

**John T. Batina
NASA Langley Research Center
Hampton, Virginia 23665-5225**

Abstract

The development of a gridless computational fluid dynamics (CFD) method for the solution of the two-dimensional Euler and Navier-Stokes equations is described. The method uses only clouds of points and does not require that the points be connected to form a grid as is necessary in conventional CFD algorithms. The gridless CFD approach appears to resolve the problems and inefficiencies encountered with structured or unstructured grid methods, and consequently offers the greatest potential for accurately and efficiently solving viscous flows about complex aircraft configurations. The method is described in detail and calculations are presented for standard Euler and Navier-Stokes cases to assess the accuracy and efficiency of the capability.

Introduction

Considerable progress in developing computational fluid dynamics (CFD) methods for aerodynamic analysis has been made over the past two decades.¹ The majority of work that has been done in CFD over the years has been on developing methods for use on computational grids that have an underlying geometrical structure and thus the grids are referred to as “structured”. For example, Fig. 1(a) shows a structured grid for the NACA 0012 airfoil. The grid is of C-type topology, has 159 points in the wraparound direction, and 49 points in the outward direction. Methods developed for structured grids have been applied to a wide variety of geometrical configurations ranging from simple, analytically defined airfoil sections such as the NACA 0012 airfoil to complex aircraft configurations such as the F-16A

fighter.² Although applications of structured grid methods to complex configurations are indeed possible they generally require more sophisticated meshing methodologies such as blocked, patched, chimera, or hybrid-type grids. For example, the F-16A fighter calculations reported in Ref. 2, which included the engine inlet and boundary layer diverter as well as the wing, fuselage, and tail in the geometrical modeling, used 27 blocks of structured cells to make up the grid. These more sophisticated meshing methodologies, in turn, significantly complicate the solution algorithms of the structured grid methods.

An alternative approach is the use of unstructured grids.³⁻⁷ In two dimensions, unstructured grids typically are constructed from triangles, and in three dimensions, they consist of tetrahedral cells. The triangles or tetrahedra may be oriented in an arbitrary way to conform to the geometry, thus making it possible to easily generate grids about very complicated shapes. Although not a complicated shape, Fig. 1(b) shows an example of an unstructured grid for the NACA 0012 airfoil. The total grid has 3300 nodes and 6466 triangles. An advantage of methods developed for unstructured grids is that they may be applied to complex aircraft configurations without having to make changes to the basic solution algorithm. Numerous calculations for complex configurations performed using various Euler codes have been reported by several researchers.³⁻⁷ However, applications to three-dimensional configurations using unstructured grid Euler codes have tended to be inefficient because the meshes have an excessively large number of cells. The excessive number of cells is due, in part, to the current state-of-the-art in generation of unstructured tetrahedral grids, which produces meshes that are much finer in the spanwise direction (for a given streamwise density) than is necessary for accurate flow computation. To alleviate the problem, the cells may be stretched in the spanwise direction when generating the mesh to reduce the number of cells. However, the stretching can create convergence and accuracy problems for the flow solver. The basic problem is that the tetrahedron is an inefficient geometrical shape (whereas the triangle tends to be an efficient shape in two dimensions). A more efficient shape for an isolated wing application is a prismatic cell defined by a polyhedron with a triangular cross-section. A mesh of this type uses triangles which form prisms when connected in the spanwise direction to grid the planes of the airfoil sections of the wing. This approach, though, not only puts structure back into the mesh it is not generally applicable to complex three-dimensional configurations.

Another problem with the unstructured-grid methodology is encountered in extending the methods for solving the Euler equations to the solution of the Navier-Stokes equations, especially in three dimensions. For viscous applications, grids generally need to be fine near the body in the outward direction to resolve the boundary layer but less fine in the direction along the surface of the body. This naturally leads to cells of high aspect ratio which tends to exacerbate the inefficiency of three-dimensional solution algorithms based on tetrahedra. Specifically, the use of tetrahedra for viscous flow applications results in an unreasonably large number of cells. The number of cells is in fact absurdly large in comparison to grids that are generated for Euler calculations (which are already inefficient because of a large number of cells as previously discussed) because of the additional requirement that the mesh be fine near the body. To alleviate this problem, a hybrid approach has been developed recently using prismatic cells for the solution of the Navier-Stokes equations.⁸ In this approach, the surface of the geometry under consideration and the outer boundaries of the mesh are gridded using triangles, and instead of generating tetrahedra to fill the interior of the computational domain, the triangles on the inner and outer boundaries of the mesh are connected to form prisms. The prisms, of course, require the same number of triangles on the inner and outer boundaries. While this hybrid approach is a viable solution to alleviate the inefficiency created by using tetrahedral cells to solve the Navier-Stokes equations, it is not necessarily the best approach, since it again puts structure back into the mesh and limits some of the advantages of the unstructured grid methodology, such as spatial adaption.

What is truly required to advance the CFD technology to treat complex configurations in viscous flows is not to take a step backward toward grid structure, but to take a bold step forward to develop methods that do not require the use of grids at all. Hence the solution to the above-mentioned problems with structured and unstructured grids is the development of algorithms for solving the Navier-Stokes equations based on using only grid points and not on the connectivity information that relates all of the points to one another. This type of approach, which may be referred to as “gridless” CFD, has distinct advantages over methods that require grids. Since only points are required, or specifically clouds of points as suggested by Chakravarthy,⁹ gridless CFD methods offer the greatest potential for accurately and efficiently solving viscous flows about complex aircraft configurations. It is noted parenthetically,

that if finally the grid points too were not required by the solution algorithm, then the ultimate flexibility in methodology could be attained. This type of method might then be referred to as “pointless” CFD.

The purpose of the paper is to report the development of a gridless method for the solution of the two-dimensional Euler and Navier-Stokes equations. The method uses only clouds of points and does not require that the points be connected to form a grid as is necessary in conventional CFD algorithms. The governing partial differential equations (PDEs) are solved directly, by performing local least-squares curve fits in each cloud of points, and then analytically differentiating the resulting curve-fit equations to approximate the derivatives of the PDEs. The method is neither a finite-difference nor a finite-volume type approach since differences, metrics, lengths, areas, or volumes are not computed. The method is described in further detail and calculations are presented for standard cases to assess the accuracy and efficiency of the capability.

Governing Equations

In this study the flow is assumed to be governed by the two-dimensional laminar Navier-Stokes equations which may be written in differential form as

$$\frac{\partial Q}{\partial t} + \frac{\partial}{\partial x}(E - E_v) + \frac{\partial}{\partial y}(F - F_v) = 0 \quad (1)$$

where Q is the vector of conserved variables given by

$$Q = \begin{pmatrix} \rho \\ \rho u \\ \rho v \\ e \end{pmatrix}$$

E and F are the inviscid fluxes in the x and y directions, respectively, defined by

$$E = \begin{pmatrix} \rho u \\ \rho u^2 + p \\ \rho uv \\ (e + p)u \end{pmatrix}$$

$$F = \begin{pmatrix} \rho v \\ \rho uv \\ \rho v^2 + p \\ (e + p)v \end{pmatrix}$$

and E_v and F_v are the viscous fluxes in the x and y directions, respectively, defined by

$$E_v = \begin{Bmatrix} 0 \\ \tau_{xx} \\ \tau_{xy} \\ u\tau_{xx} + v\tau_{xy} - q_x \end{Bmatrix}$$

$$F_v = \begin{Bmatrix} 0 \\ \tau_{xy} \\ \tau_{yy} \\ u\tau_{xy} + v\tau_{yy} - q_y \end{Bmatrix}$$

In the viscous fluxes the shear stresses and heat flux terms are defined by

$$\tau_{xx} = \frac{2}{3} \frac{M_\infty}{Re} \mu \left(2 \frac{\partial u}{\partial x} - \frac{\partial v}{\partial y} \right)$$

$$\tau_{yy} = \frac{2}{3} \frac{M_\infty}{Re} \mu \left(2 \frac{\partial v}{\partial y} - \frac{\partial u}{\partial x} \right)$$

$$\tau_{xy} = \frac{M_\infty}{Re} \mu \left(\frac{\partial u}{\partial y} + \frac{\partial v}{\partial x} \right)$$

$$q_x = -\frac{\gamma}{\gamma - 1} \frac{M_\infty}{Re Pr} \mu \frac{\partial}{\partial x} \left(\frac{p}{\rho} \right)$$

$$q_y = -\frac{\gamma}{\gamma - 1} \frac{M_\infty}{Re Pr} \mu \frac{\partial}{\partial y} \left(\frac{p}{\rho} \right)$$

In these equations, M_∞ is the freestream Mach number, Re is the Reynolds number, Pr is the Prandtl number, and μ is the molecular viscosity determined using Sutherland's law. The Euler equations are obtained by setting the viscous fluxes equal to zero.

Spatial Discretization

Derivatives

The spatial derivatives in the governing equations (Eq. (1)) are approximated as follows. In each cloud of points, each term of the fluxes is assumed to vary linearly according to

$$f(x, y) = a_0 + a_1 x + a_2 y \quad (2)$$

where the coefficients a_0 , a_1 , and a_2 are determined from a least-squares curve fit. Performing a least-squares fit in a given cloud results in three equations represented in matrix form by

$$\begin{bmatrix} n & \Sigma x_i & \Sigma y_i \\ \Sigma x_i & \Sigma x_i^2 & \Sigma x_i y_i \\ \Sigma y_i & \Sigma x_i y_i & \Sigma y_i^2 \end{bmatrix} \begin{Bmatrix} a_0 \\ a_1 \\ a_2 \end{Bmatrix} = \begin{Bmatrix} \Sigma f_i \\ \Sigma x_i f_i \\ \Sigma y_i f_i \end{Bmatrix} \quad (3)$$

where n is the number of points in the cloud and the summations are taken over the n points. The solution of Eqs. (3) requires the inversion of a 3×3 matrix which is performed for every cloud in the computational domain. Having solved these equations for a_0 , a_1 , and a_2 , the spatial derivatives are now known since by differentiating Eq. (2) it is obvious that

$$\frac{\partial f}{\partial x} = a_1 \quad \frac{\partial f}{\partial y} = a_2 \quad (4)$$

In addition to approximating the spatial derivatives of the governing equations by differentiation of the least-squares curve fits, the shear stresses and heat flux terms are calculated the same way. Since these terms involve first derivatives of the velocity components or pressure divided by density, the shear stresses and heat fluxes can be approximated by defining f to be equal to u , v , or p/ρ , evaluating the terms of Eqs. (3), and inverting the left-hand-side matrix. The resulting values for a_1 and a_2 are the derivatives of the specified quantity with respect to x and y , respectively, within a given cloud of points.

Artificial Dissipation

The unsteady Euler equations are a set of nondissipative hyperbolic conservation laws that require some form of artificial dissipation to prevent oscillations near shock waves and to damp high-frequency uncoupled error modes. The unsteady Navier-Stokes equations also require artificial dissipation for similar reasons because the physical viscosity generally is limited to the boundary layer. Since the method of the present work is conceptually analogous to a central-difference type approach, the artificial dissipation must be added explicitly to the solution procedure. This is accomplished by adding harmonic and biharmonic terms to the governing equations, corresponding to second and fourth differences of the conserved variables, respectively. These dissipation terms are defined by

$$D = \nabla \left(\epsilon^{(2)} \lambda \right) \nabla Q - \nabla^2 \left(\epsilon^{(4)} \lambda \right) \nabla^2 Q \quad (5)$$

where λ is the local maximum eigenvalue of the governing equations, and $\epsilon^{(2)}$ and $\epsilon^{(4)}$ are local dissipation coefficients that are formulated similar to those of Jameson.¹ Furthermore, the above treatment of the artificial dissipation constitutes an isotropic dissipation model (independent of coordinate direction) which generally is only applicable to the Euler equations. For the Navier-Stokes equations, an anisotropic model

is required due in part to the close spacing of points normal to the surface relative to the tangential distribution of points (analogous to high aspect ratio cells in structured or unstructured grid methods). Thus an anisotropic dissipation model was developed for use when solving the Navier-Stokes equations on clouds of points.

Temporal Discretization

Time Integration

The governing flow equations are integrated numerically in time using an explicit multi-stage Runge-Kutta time-stepping scheme.¹ Typically a four-stage scheme is used to solve the Euler equations with the artificial dissipation evaluated only during the first stage. A five-stage scheme is used to solve the Navier-Stokes equations with the artificial dissipation evaluated during the first, third, and fifth stages.

Residual Smoothing

The Runge-Kutta time-integration scheme described in the previous section has a step size that is limited by the Courant-Friedricks-Lewy (CFL) condition corresponding to CFL numbers of approximately 2.8 and 3.6 for the four-stage and five-stage schemes, respectively. To accelerate convergence to steady state, the CFL number may be increased by averaging the residual R with values at neighboring points.¹ This is accomplished by replacing R by the smoothed residual \bar{R} given by

$$\bar{R} - \epsilon \nabla^2 \bar{R} = R \quad (6)$$

where ϵ is a constant which controls the amount of smoothing and ∇^2 is a harmonic operator similar to that used in the dissipation model. Also similar to the dissipation model, an anisotropic form of the harmonic operator is used when solving the Navier-Stokes equations. Equation (6) is solved approximately using several Jacobi iterations. Convergence to steady state is further accelerated using enthalpy damping (only for the Euler equations) and local time stepping.

Boundary Conditions

To impose the boundary conditions along the surface of the geometry being considered, ghost points that are located inside of the geometry are used. The locations of these ghost points are determined by

a simple reflection of the flow field points that are close to the surface about the edges that define the boundary. A similar procedure is used near the outer boundary to determine the locations of ghost points at which to impose the far-field boundary conditions.

Along solid surfaces, the velocity components at the ghost points are determined from the values at the corresponding flow field point adjacent to the surface. When solving the Euler equations, the velocity components at the ghost points are determined by imposing a flow tangency or slip condition which requires that the velocity normal to the surface vanishes. When solving the Navier-Stokes equations, the velocity components at the ghost points are determined by imposing a no-slip condition which simply changes the sign of the values of the components at the adjacent flow field points. In either case (Euler or Navier-Stokes), pressure and density at the ghost points are set equal to the values at the adjacent flow field points. Additional conditions are imposed using the ghost points to accurately treat the shear stresses and heat flux terms, as well as the artificial dissipation terms.

In the far field a characteristic analysis based on Riemann invariants is used to determine the values of the inviscid flow variables at the ghost points that are located outside of the outer boundary. This analysis correctly accounts for wave propagation in the far field which is important for rapid convergence to steady state. Values of the viscous flow quantities at these ghost points are set equal to the values at the corresponding flow field points adjacent to the outer boundary.

Results and Discussion

Calculations were performed first with the Euler equations and then with the Navier-Stokes equations, to assess the feasibility of the gridless CFD concept. The results were obtained for standard cases to determine the accuracy and efficiency of the methodology. All of the results were obtained on the Cray-YMP computer (Reynolds) at the Numerical Aerodynamic Simulation Facility located at the NASA Ames Research Center.

Euler Results

Results were obtained first by solving the Euler equations for flows about the NACA 0012 airfoil. The field of points that was used to model the flow about the airfoil is plotted in Fig. 2. For convenience,

the locations of these points were determined by using the cell centers from the unstructured grid of Fig. 1(b), and the cloud of points for each point was taken to be the cell centers of the three triangles that share edges with a given triangle. To more clearly demonstrate this, Fig. 3(a) shows a close-up view of the unstructured grid near the airfoil nose, and Fig. 3(b) shows the points determined from the cell centers. Figure 3(b) also shows ghost points that are located inside of the airfoil in order to impose the surface boundary conditions. The computational domain has a total of 6,500 points, 134 of which are ghost points. It is emphasized that the unstructured grid of Fig. 1(b) was used to determine the field of points of Fig. 2 only for convenience. In general, any method to determine the points is acceptable. Efficient generation procedures to determine clouds of points have yet to be developed.

Euler results were obtained using the points of Fig. 2 for four standard NACA 0012 airfoil cases corresponding to various combinations of freestream Mach number M_∞ and angle of attack α including: (1) $M_\infty = 0.8$, $\alpha = 0^\circ$; (2) $M_\infty = 0.85$, $\alpha = 1^\circ$; (3) $M_\infty = 0.8$, $\alpha = 1.25^\circ$; and (4) $M_\infty = 1.2$, $\alpha = 7^\circ$. All four cases were run using a CFL number of 5.0 with local time-stepping, residual smoothing, and enthalpy damping to accelerate convergence to steady state. Figure 4 shows the resulting convergence histories plotted as the log of the L_2 -norm of the density residual versus the CPU time in minutes. The convergence histories indicate that convergence to steady state is obtained in only several minutes of CPU time; thus, the method is reasonably efficient in comparison with accepted runtimes of more conventional Euler methods (without multigrid acceleration). As further shown in Fig. 4, the slowest convergence is for case 2 ($M_\infty = 0.85$, $\alpha = 1^\circ$), which is because the solution contains two shock waves (upper and lower surfaces of the airfoil) of moderate strength. Therefore, it is slightly harder to converge the solution of case 2 in comparison with the solutions of the other cases. Figure 5 shows the corresponding pressure coefficient distributions C_p versus the fractional chordlength x/c for the four NACA 0012 airfoil cases. The pressure distributions for cases 1, 2, and 3 indicate that the shock waves are sharply captured with only one interior point, which is somewhat surprising for a method that corresponds essentially to central differencing. The pressures for all four cases indicate that the generally accepted Euler solutions have been obtained, which suggests that the gridless CFD method is accurate as well as efficient for such applications.

Navier-Stokes Results

Next, results were obtained by solving the Navier-Stokes equations first for a flat plate and then for the NACA 0012 airfoil. For the flat plate, a solution was obtained initially to assess the gridless Navier-Stokes capability by making comparisons with the exact Blasius solution. The field of points used in these calculations was generated from a structured mesh of grid points, that were uniformly distributed along the flat plate but clustered near the plate in the normal direction to resolve the boundary layer. The calculations were performed for $M_\infty = 0.5$ and $Re = 10,000$. The resulting streamwise velocity component u (normalized by the freestream value u_e), plotted versus the similarity variable $(y/x)\sqrt{Re}$, is shown in Fig. 6 at $x/l = 0.233, 0.383, 0.533, 0.683,$ and 0.833 . The gridless results, represented by the symbols, indicate that the similarity solution for a flat plate boundary layer is correctly obtained and that the solution agrees well with the Blasius solution.

Navier-Stokes results were also obtained for a standard laminar case for the NACA 0012 airfoil corresponding to $M_\infty = 0.5$, $\alpha = 0^\circ$, and $Re = 5000$. The field of points that was used to model the flow about the airfoil was again determined for convenience by using the cell centers from an unstructured grid of triangles. A partial view of the unstructured grid is shown in Fig. 7(a) (generated from a structured grid of C-type topology), and the corresponding view of points for the gridless method is shown in Fig. 7(b). Close-up views near the airfoil nose of the unstructured grid and the gridless field of points are shown in Figs. 8(a) and 8(b), respectively. The computational domain in the latter case has a total of 30,720 points, 608 of which are ghost points. Navier-Stokes results were obtained using a CFL number of 4.0 with local time-stepping and residual smoothing to accelerate convergence to steady state. Figure 9(a) shows the resulting convergence history plotted as the log of the L_2 -norm of the density residual versus the CPU time in minutes. The convergence history indicates that acceptable convergence is obtained in less than one hour of CPU time which is reasonable considering that the method does not currently use multigrid to accelerate convergence to steady state. Figure 9(b) shows the corresponding pressure distribution which indicates that the generally accepted Navier-Stokes solution involving separated flow near the trailing edge has been obtained by using the gridless CFD method. To

more clearly see the flow solution in the trailing-edge region, velocity vectors are presented in Fig. 10. The flow separates near 82% chord along the upper and lower surfaces of the airfoil, and the velocity vectors indicate that there are small recirculation bubbles downstream of the trailing edge. This solution is consistent with the Navier-Stokes solutions reported by other researchers obtained for this case using structured (Ref. 10) and unstructured (Ref. 11) grids.

Concluding Remarks

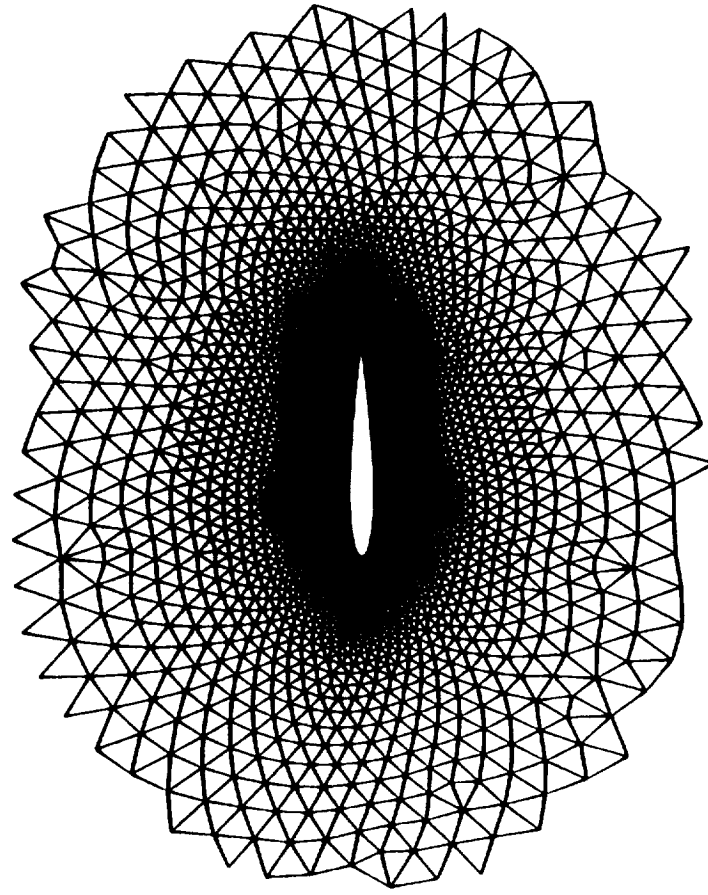
The development of a gridless CFD method for the solution of the two-dimensional Euler and Navier-Stokes equations was described. The method uses only clouds of points and does not require that the points be connected to form a grid as is necessary in conventional CFD algorithms. The gridless CFD approach appears to resolve the problems and inefficiencies encountered with structured or unstructured grid methods and, consequently, offers the greatest potential for accurately and efficiently solving viscous flows about complex aircraft configurations. The method was described in detail and calculations for standard cases were presented to assess the accuracy and efficiency of the capability. The capability was tested for the solution of the Euler equations and for the solution of the laminar Navier-Stokes equations. These solutions were found to be accurate and efficient in comparison with solutions from conventional CFD methods.

Future Work

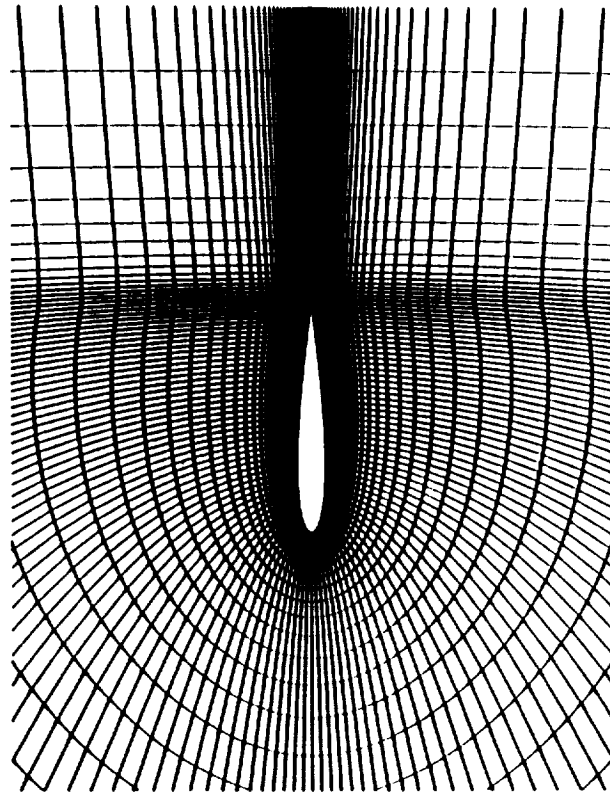
The three-dimensional version of the gridless algorithm has been developed for the solution of the Euler and Navier-Stokes equations and is currently being evaluated for three-dimensional applications. An Euler case that is being considered is a transonic flow about the Boeing 747 transport configuration. For convenience, a field of points has been created from an existing unstructured mesh of tetrahedra for the 747, using the cell centers to locate the points for use by the gridless method. The computational domain contains 109,805 points, 8,330 of which are ghost points. The ghost points that are being used to model the surface of the 747 are shown in Fig. 11. These ghost points clearly show that the geometry includes the fuselage, the wings, horizontal and vertical tails, underwing pylons, and flow-through engine nacelles.

References

1. Jameson, A.: Successes and Challenges in Computational Aerodynamics, AIAA Paper No. 87-1184, January 1987.
2. Flores, J.; and Chaderjian, N. M.: Zonal Navier-Stokes Methodology for Flow Simulation About a Complete Aircraft, Journal of Aircraft, vol. 27, July 1990, pp. 583-590.
3. Jameson, A.; Baker, T. J.; and Weatherill, N. P.: Calculation of Inviscid Transonic Flow over a Complete Aircraft, AIAA Paper No. 86-0103, January 1986.
4. Peraire, J.; Peiro, J.; Formaggia, L.; and Morgan, K.: Finite Element Euler Computations in Three Dimensions, AIAA Paper No. 88-0032, January 1988.
5. Lohner, R.; and Baum, J. D.: Numerical Simulation of Shock Interaction with Complex Geometry Three-Dimensional Structures Using a New Adaptive H-Refinement Scheme on Unstructured Grids, AIAA Paper No. 90-0700, January 1990.
6. Frink, N. T.; Parikh, P.; and Pirzadeh, S.: Aerodynamic Analysis of Complex Configurations Using Unstructured Grids, AIAA Paper No. 91-3292, September 1991.
7. Batina, J. T.: A Fast Implicit Upwind Solution Algorithm for Three Dimensional Unstructured Dynamic Meshes, AIAA Paper No. 92-0447, January 1992.
8. Nakahashi, K.: A Finite-Element Method on Prismatic Elements for the Three-Dimensional Navier-Stokes Equations, Lecture Notes in Physics, Springer-Verlag, vol. 323, 1989, pp. 434-438.
9. Chakravarthy, S. R.: Some New Approaches to Grid Generation, Discretization, and Solution Methods for CFD, presented at the 4th International Symposium on Computational Fluid Dynamics, Davis, California, September 9-12, 1991.
10. Radespiel, R.; and Swanson, R. C.: An Investigation of Cell Centered and Cell Vertex Multigrid Schemes for the Navier-Stokes Equations, AIAA Paper No. 89-0543, January 1989.
11. Mavriplis, D. J.; Jameson, A.; and Martinelli, L.: Multigrid Solution of the Navier-Stokes Equations on Triangular Meshes, ICASE Report No. 89-11, February 1989.



(b) unstructured.



(a) structured.

Fig. 1 Partial view of meshes about the NACA 0012 airfoil.

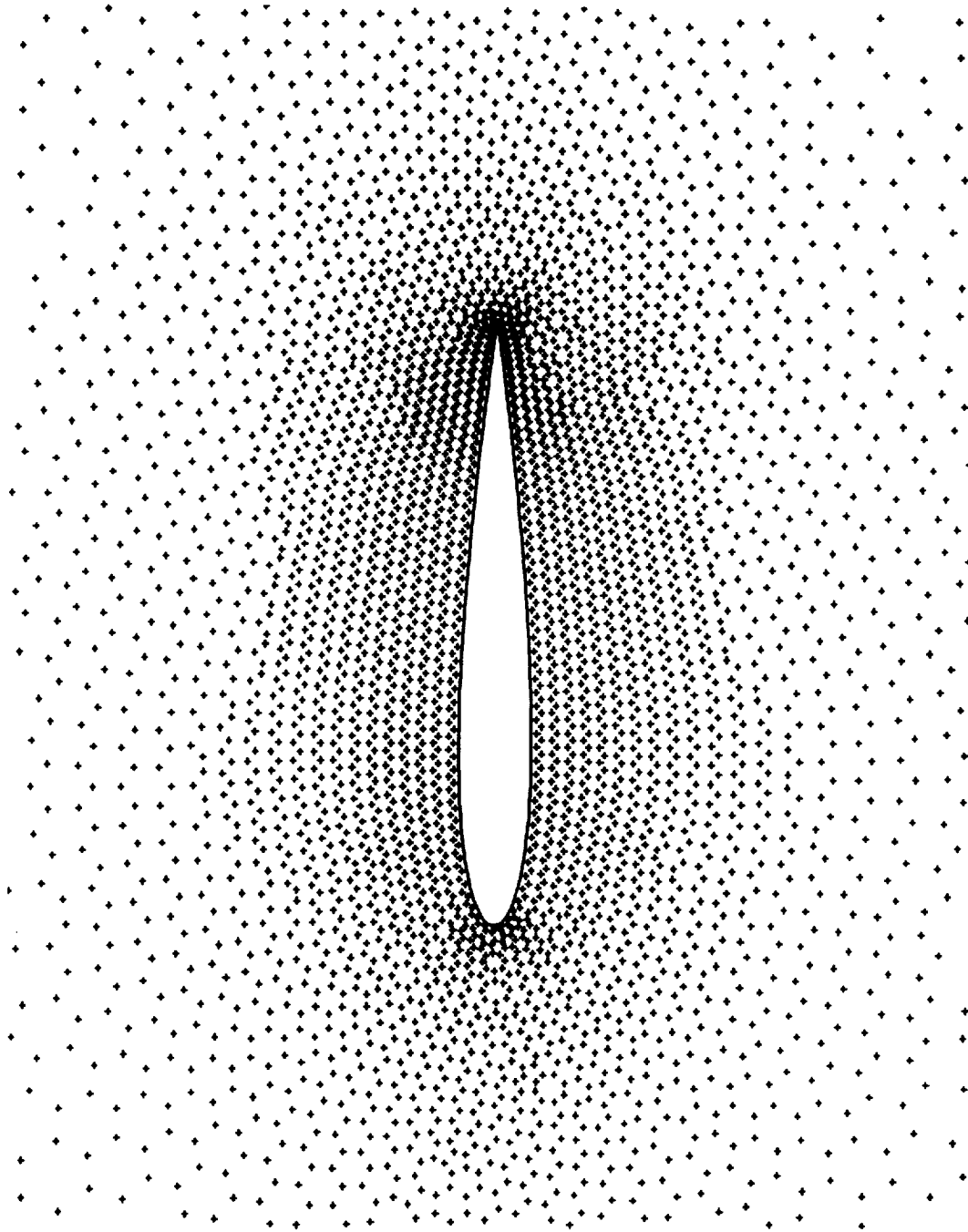
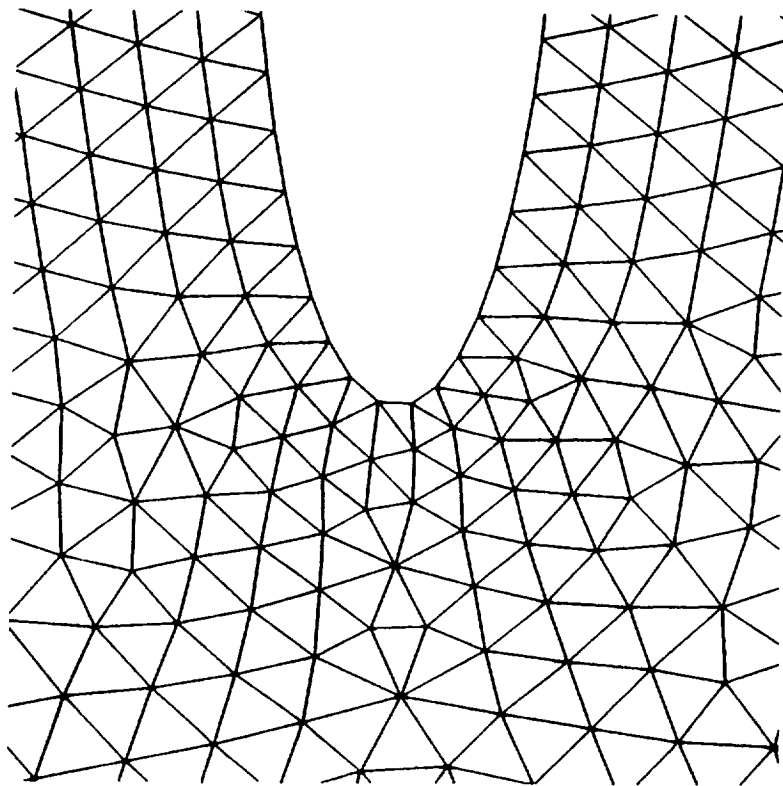
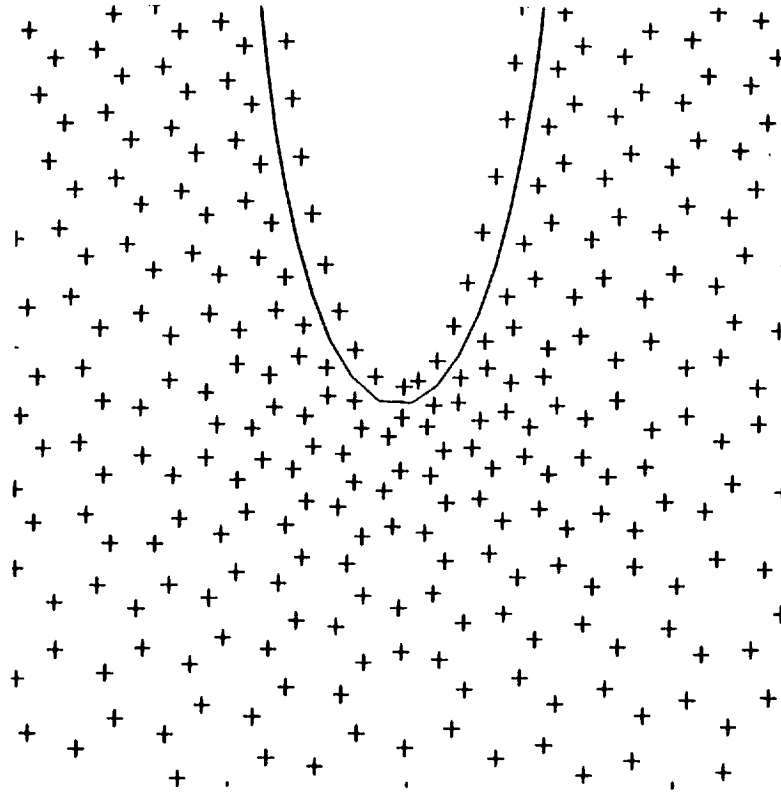


Fig. 2 Partial view of field of points about the NACA 0012 airfoil.



(a) unstructured mesh of triangles.



(b) corresponding field of points and ghost points for boundary conditions.

Fig. 3 Close-up view near the nose of the NACA 0012 airfoil.

1. $M_\infty = 0.8, \alpha = 0^\circ$
2. $M_\infty = 0.85, \alpha = 1^\circ$
3. $M_\infty = 0.8, \alpha = 1.25^\circ$
4. $M_\infty = 1.2, \alpha = 7^\circ$

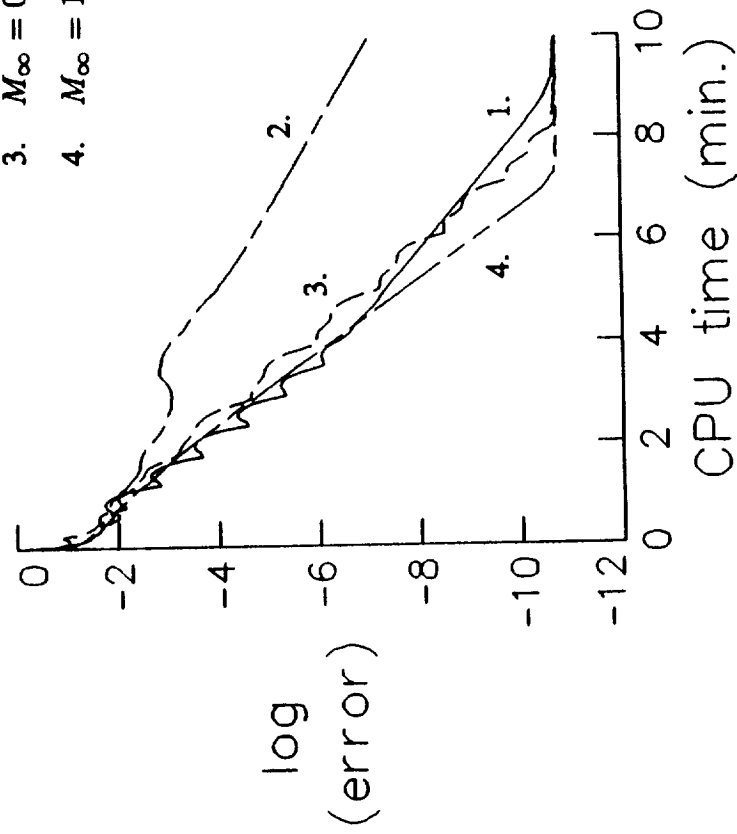


Fig. 4 Convergence histories from the gridless Euler solutions for the NACA 0012 airfoil.

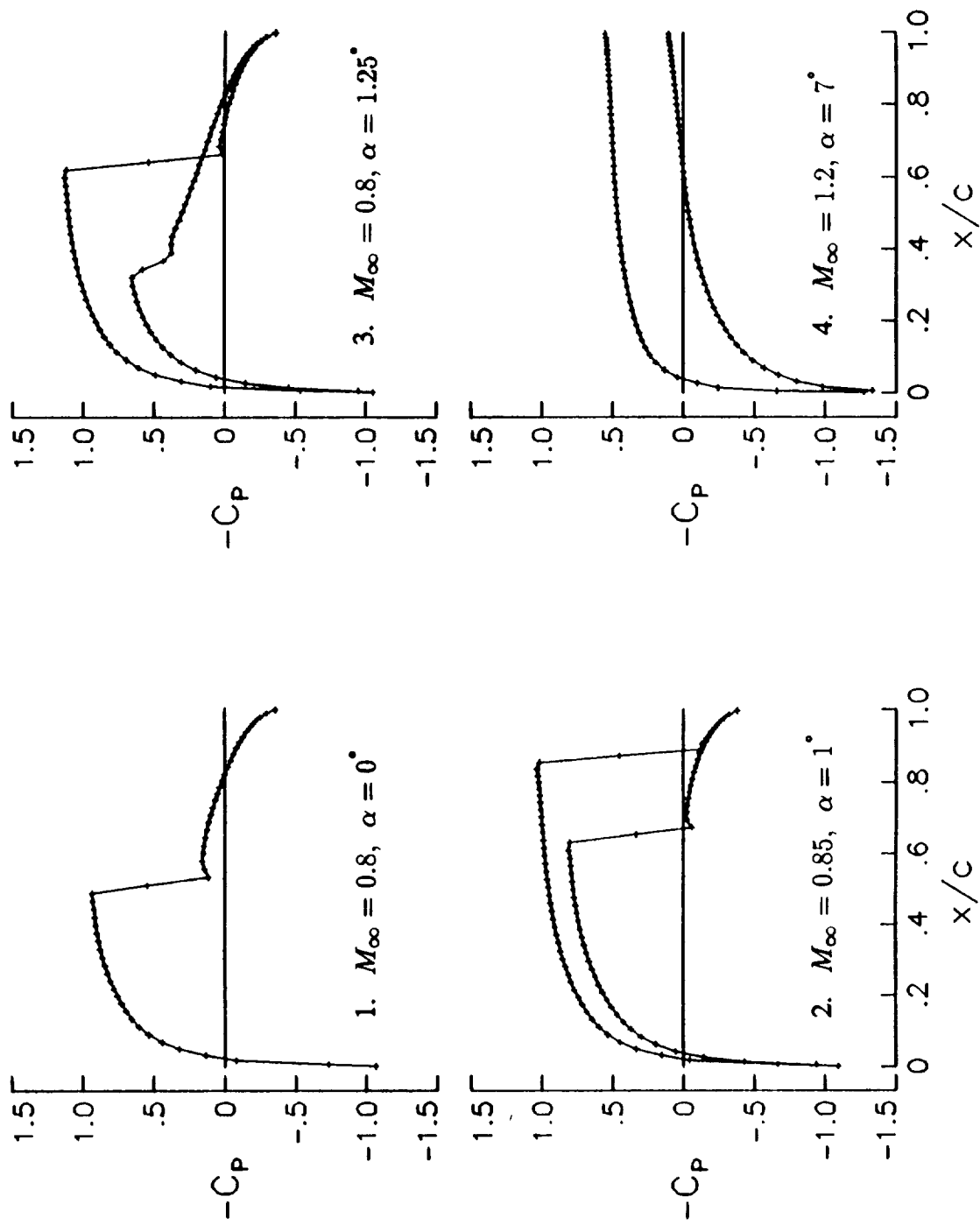


Fig. 5 Pressure distributions from the gridless Euler solutions for the NACA 0012 airfoil.

This page left intentionally blank.

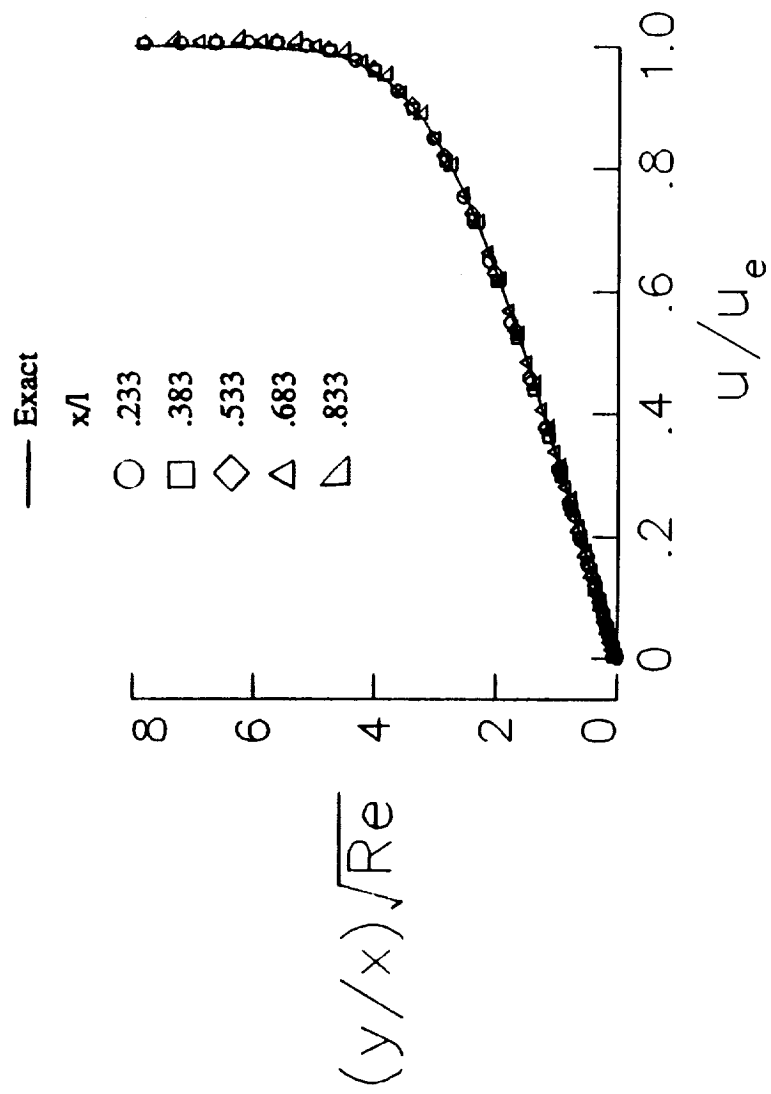
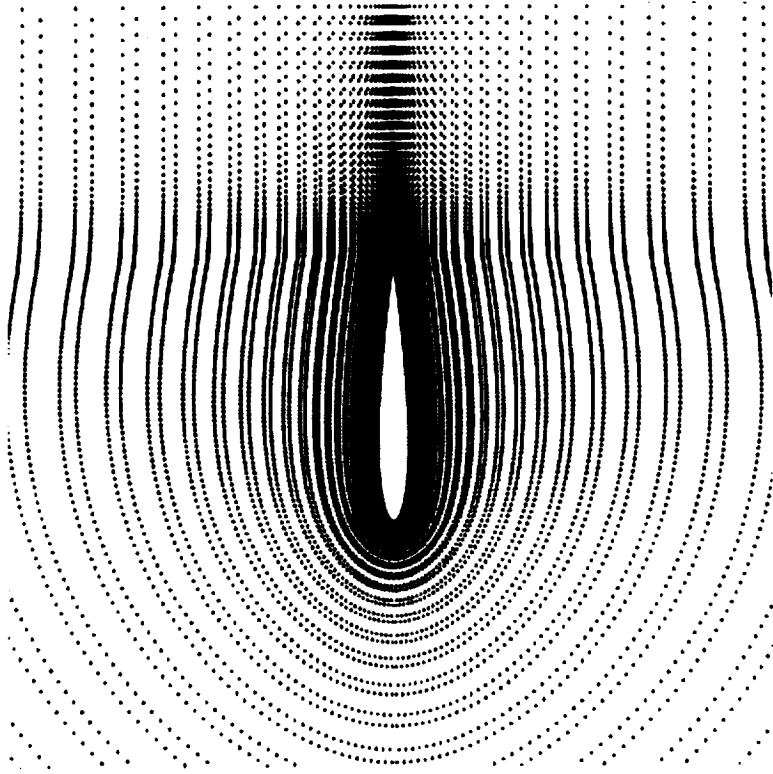
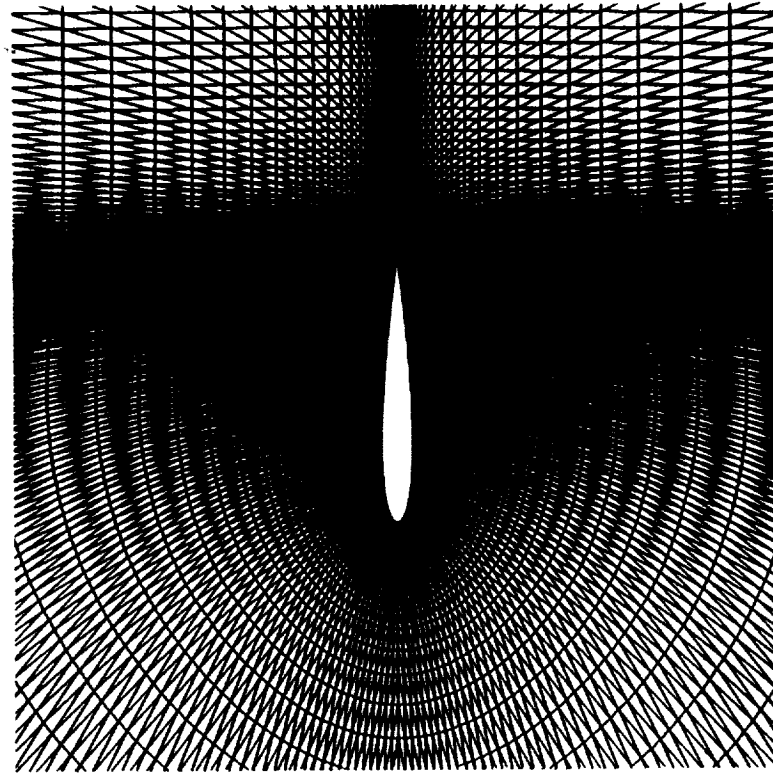


Fig. 6 Streamwise velocity distribution from the gridless Navier-Stokes solution for a flat plate at $M_\infty = 0.5$ and $Re = 10,000$.

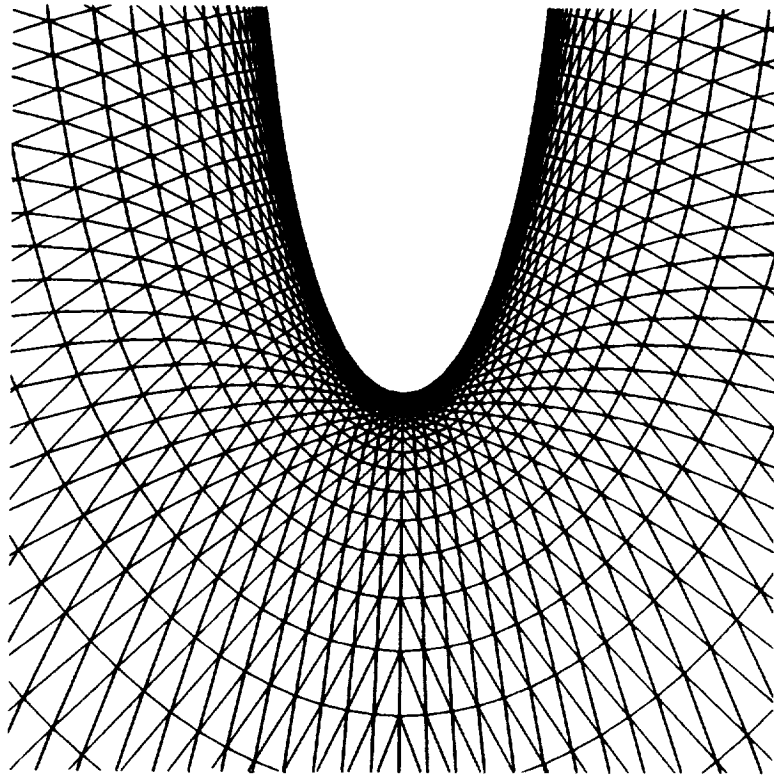


(b) corresponding field of points.

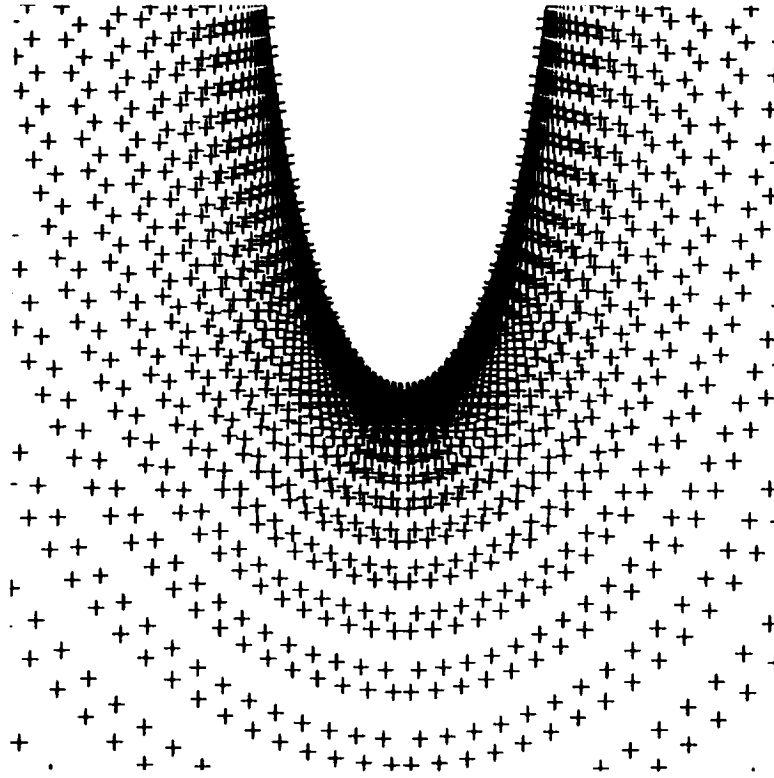


(a) unstructured mesh of triangles.

Fig. 7 Partial view of computational domains for the NACA 0012 airfoil.

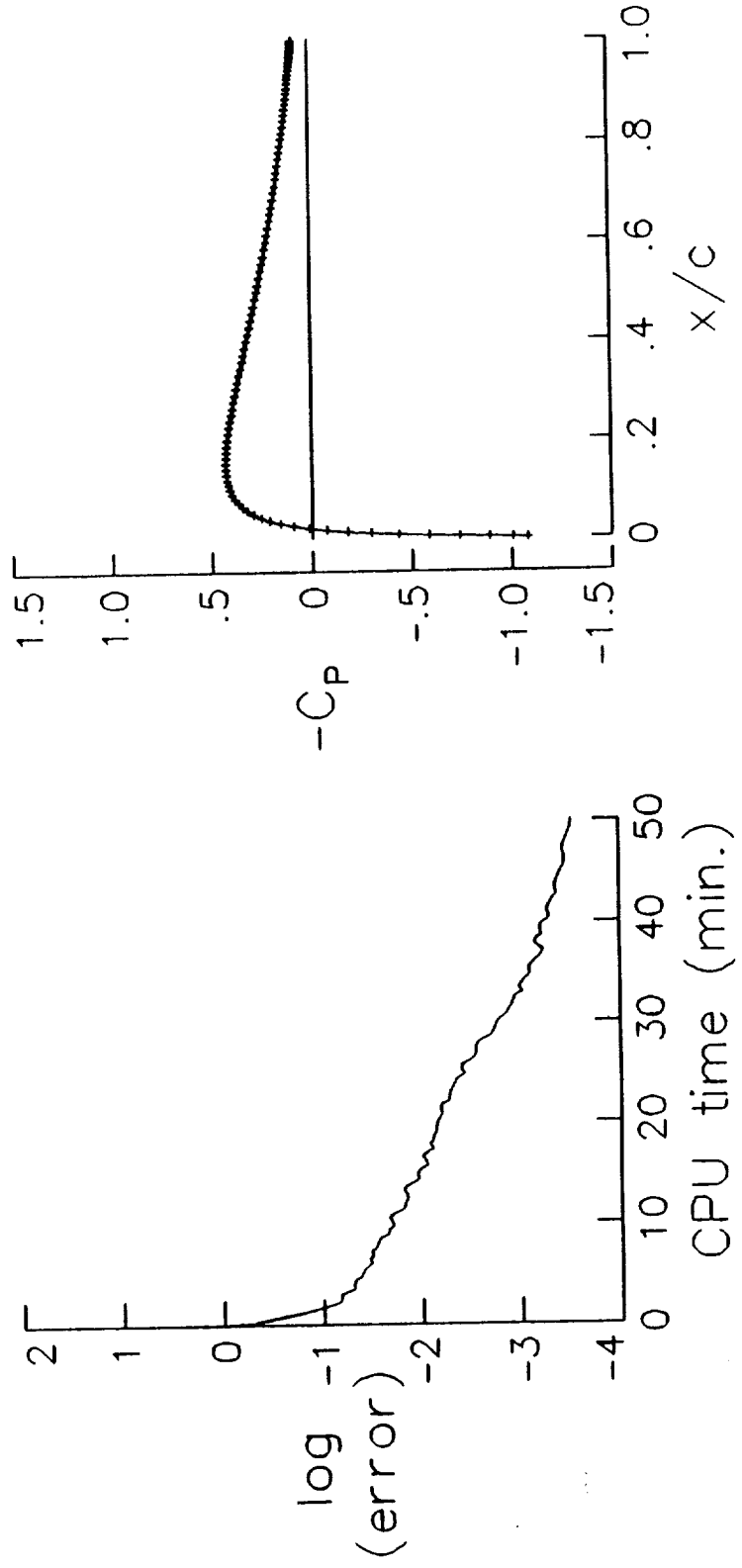


(a) unstructured mesh of triangles.



(b) corresponding field of points.

Fig. 8 Close-up view near the nose of the NACA 0012 airfoil.



(a) convergence history.

(b) pressure distribution.

Fig. 9 Gridless Navier-Stokes solution for the NACA 0012 airfoil at $M_\infty = 0.5$, $\alpha = 0^\circ$, and $Re = 5000$.

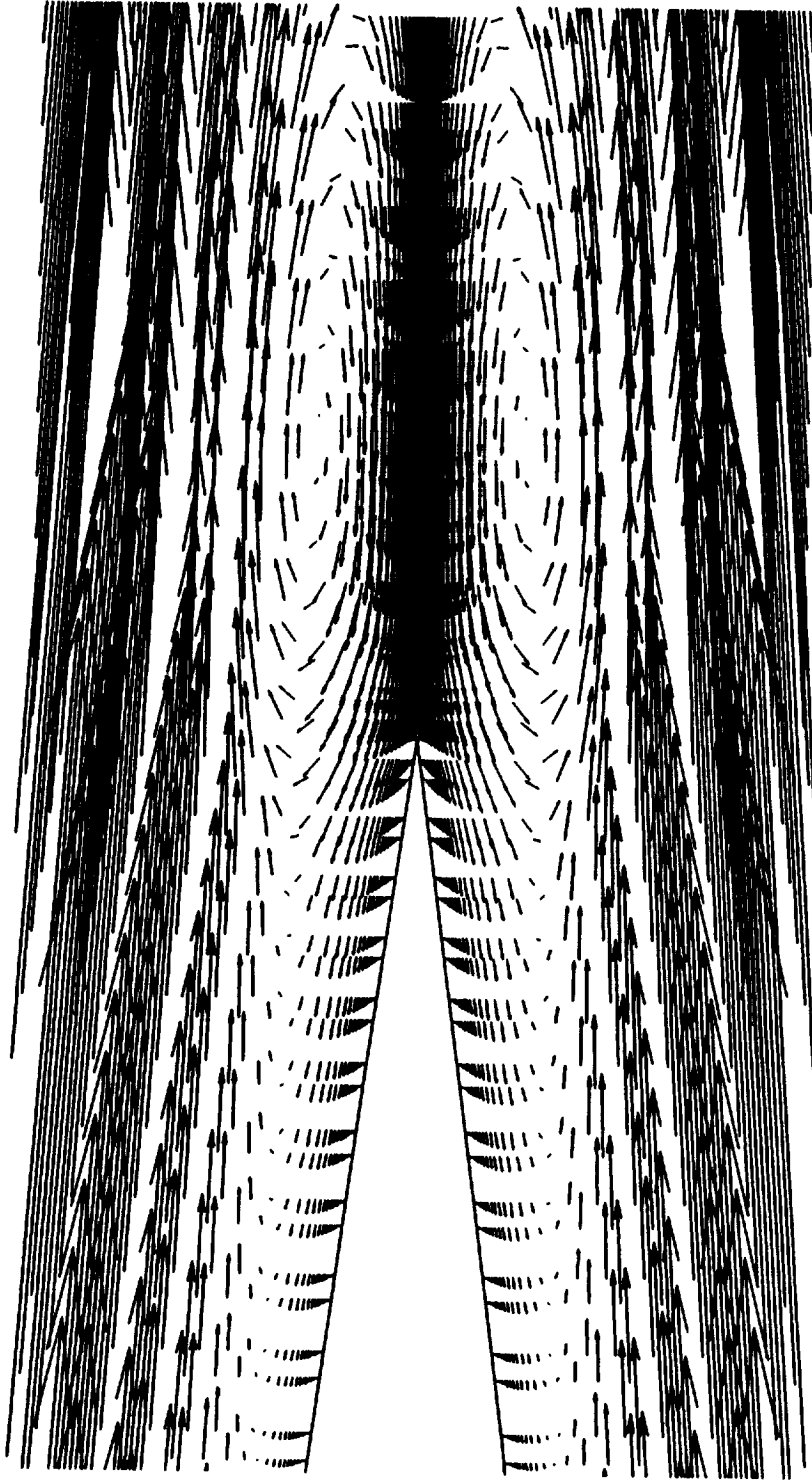


Fig. 10 Velocity vectors near the trailing edge of the NACA 0012 airfoil at $M_\infty = 0.5$, $\alpha = 0^\circ$, and $Re = 5000$.

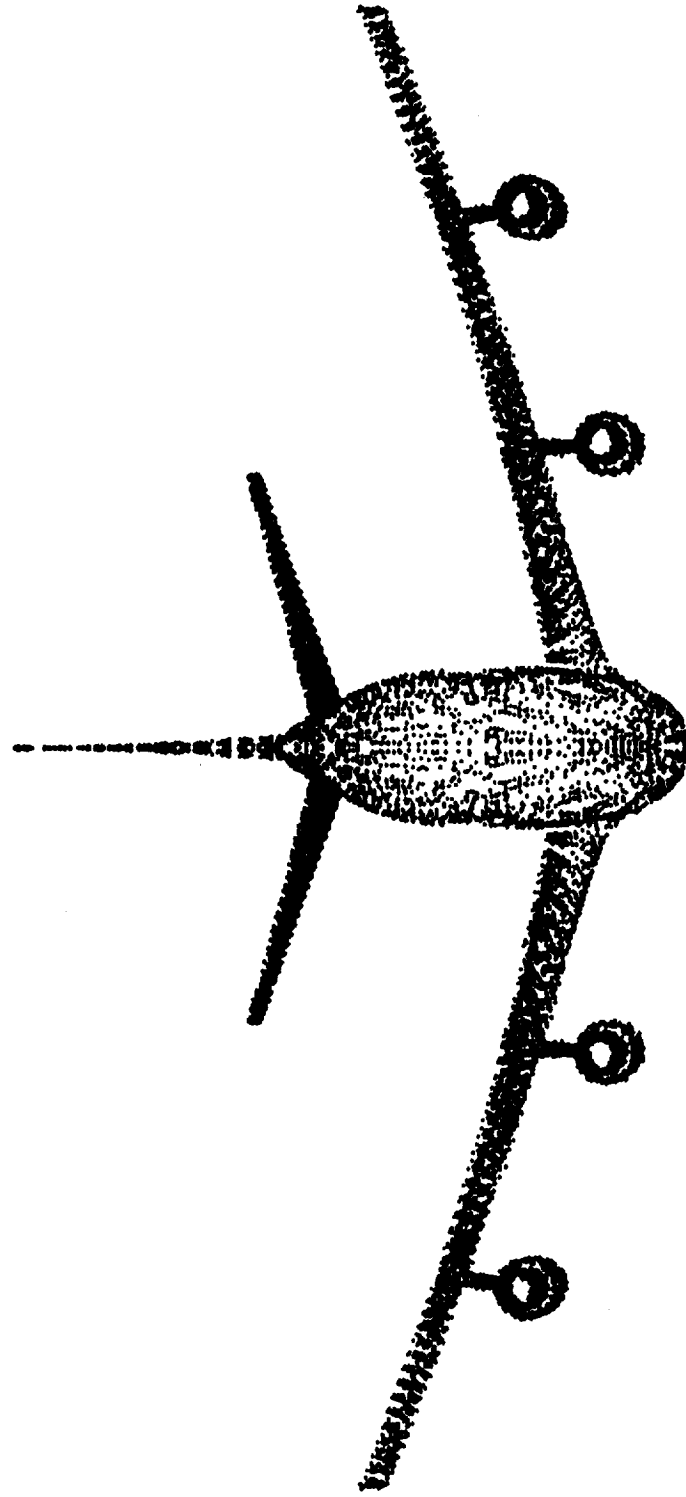


Fig. 11 Ghost points for the Boeing 747 transport configuration.

REPORT DOCUMENTATION PAGE

Form Approved
OMB No. 0704-0188

Public reporting burden for this collection of information is estimated to average 1 hour per response, including the time for reviewing instructions, searching existing data sources, gathering and maintaining the data needed, and completing and reviewing the collection of information. Send comments regarding this burden estimate or any other aspect of this collection of information, including suggestions for reducing this burden, to Washington Headquarters Services, Directorate for Information Operations and Reports, 1215 Jefferson Davis Highway, Suite 1204, Arlington, VA 22202-4302, and to the Office of Management and Budget, Paperwork Reduction Project (0704-0188), Washington, DC 20503.

1. AGENCY USE ONLY (<i>Leave blank</i>)	2. REPORT DATE June 1992	3. REPORT TYPE AND DATES COVERED Technical Memorandum	
4. TITLE AND SUBTITLE A Gridless Euler/Navier-Stokes Solution Algorithm for Complex Two-Dimensional Applications		5. FUNDING NUMBERS 505-63-50-12	
6. AUTHOR(S) John T. Batina		8. PERFORMING ORGANIZATION REPORT NUMBER	
7. PERFORMING ORGANIZATION NAME(S) AND ADDRESS(ES) NASA Langley Research Center Hampton, VA 23665-5225		10. SPONSORING / MONITORING AGENCY REPORT NUMBER NASA TM 107631	
9. SPONSORING / MONITORING AGENCY NAME(S) AND ADDRESS(ES) National Aeronautics and Space Administration Washington, DC 20546-0001		11. SUPPLEMENTARY NOTES	
12a. DISTRIBUTION / AVAILABILITY STATEMENT Unclassified - Unlimited Subject Category 02		12b. DISTRIBUTION CODE	
13. ABSTRACT (<i>Maximum 200 words</i>) The development of a gridless computational fluid dynamics (CFD) method for the solution of the two-dimensional Euler and Navier-Stokes equations is described. The method uses only clouds of points and does not require that the points be connected to form a grid as is necessary in conventional CFD algorithms. The gridless CFD approach, appears to resolve the problems and inefficiencies encountered with structured or unstructured grid methods, and consequently offers the greatest potential for accurately and efficiently solving viscous flows about complex aircraft configurations. The method is described in detail and calculations are presented for standard Euler and Navier-Stokes cases to assess the accuracy and efficiency of the capability.			
14. SUBJECT TERMS Transonic Aerodynamics Viscous Aerodynamics Computational Fluid Dynamics		15. NUMBER OF PAGES 25	16. PRICE CODE A03
17. SECURITY CLASSIFICATION OF REPORT Unclassified	18. SECURITY CLASSIFICATION OF THIS PAGE Unclassified	19. SECURITY CLASSIFICATION OF ABSTRACT Unclassified	20. LIMITATION OF ABSTRACT